RESEARCH PAPER

Prion 7:2, 185–191; March/April 2013; © 2013 Landes Bioscience

Comparison of the local structural stabilities of mammalian prion protein (PrP) by fragment molecular orbital calculations

Koji Hasegawa,[1] Shirou Mohri[2] and Takashi Yokoyama[2,*]

[1]AdvanceSoft Corporation; Tokyo, Japan; [2]Prion Disease Research Center; National Institute of Animal Health; Ibaraki, Japan

Keywords: prion, BSE, species barrier, FMO, structure

Abbreviations: BSE, bovine spongiform encephalopathy; FMO, fragment molecular orbital; IFIE, interfragment interaction energy; NMR, nuclear magnetic resonance; ΔE^{Int}, internal interaction energy; ΔE^{pair}, pair interaction energy; PCA, principal component analysis; PDB, Protein Data Bank; PrP, prion protein; PrP^{C}, cellular PrP; PrP^{Sc}, pathogenic isoform of PrP; vCJD, variant Creutzfeldt-Jakob disease

Bovine spongiform encephalopathy (BSE), a member of the prion diseases, is a fatal neurodegenerative disorder suspected to be caused by a malfunction of prion protein (PrP). Although BSE prions have been reported to be transmitted to a wide range of animal species, dogs and hamsters are known to be BSE-resistant animals. Analysis of canine and hamster PrP could elucidate the molecular mechanisms supporting the species barriers to BSE prion transmission. The structural stability of six mammalian PrPs, including human, cattle, mouse, hamster, dog and cat, was analyzed. We then evaluated intramolecular interactions in PrP by fragment molecular orbital (FMO) calculations. Despite similar backbone structures, the PrP side-chain orientations differed among the animal species examined. The pair interaction energies between secondary structural elements in the PrPs varied considerably, indicating that the local structural stabilities of PrP varied among the different animal species. Principal component analysis (PCA) demonstrated that different local structural stability exists in bovine PrP compared with the PrP of other animal species examined. The results of the present study suggest that differences in local structural stabilities between canine and bovine PrP link diversity in susceptibility to BSE prion infection.

Introduction

Bovine spongiform encephalopathy (BSE), a member of the prion diseases, is a fatal neurodegenerative disorder caused by structural conversion of cellular prion protein (PrP^{C}) into its pathogenic isoform (PrP^{Sc}).[1] However, little is known about the mechanism of this conversion. The *Prnp* gene is highly conserved among many mammalian species and PrP^{C} shows a high degree of homology among mammals, accounting for the ease of cross-species transmission of prion diseases. Several amino acids have been identified as critical for interspecies prion transmission; amino acid substitutions of these critical residues create a species barrier, resulting in diminishment or complete abolition of the efficiency of prion transmission.[2]

A wide range of host species are affected by BSE prions. Experimentally, BSE has been transmitted to mice,[3] sheep, goats,[4] minks,[5] marmosets,[6] macaques[7] and lemurs.[8] In nature, BSE has been transmitted to cattle,[9] several zoo ruminants[10] and domestic and wild cats.[11] Furthermore, BSE has been transmitted to humans via cattle, causing variant Creutzfeldt-Jakob disease (vCJD).[12] On the other hand, several species have been observed to be resistant to BSE infection. Although, no experimental result was reported regarding BSE-challenged dog. While cats were reported to develop feline spongiform encephalopathy, dogs did not appear to be affected by BSE, even after they were fed similarly infected pet food.[13] In addition, typical BSE prions were not transmitted to hamsters at primary passage.[14] Analysis of canine and hamster PrP^{C} could elucidate the molecular mechanisms accounting for the species barrier to BSE prion transmission in these species.

The three-dimensional structure of PrP^{Sc} cannot be determined directly because PrP^{Sc} is insoluble in aqueous solution and has a strong tendency to form fibrils and amorphous aggregates. It has reported that the negative charge of polyoxometalates determines the quaternary structure of PrP^{Sc} fibrils.[15] However, little is currently known about the PrP^{Sc} structures. Nuclear magnetic resonance (NMR) spectroscopy and X-ray crystallography have revealed that the three-dimensional structure of the C-terminal globular domains of PrP^{C} showed similarities among the various mammalian species examined.[16-20] It has reported that β2-α2

*Correspondence to: Takashi Yokoyama; Email: tyoko@affrc.go.jp
Submitted: 10/22/12; Revised: 11/27/12; Accepted: 12/04/12
http://dx.doi.org/10.4161/pri.23122

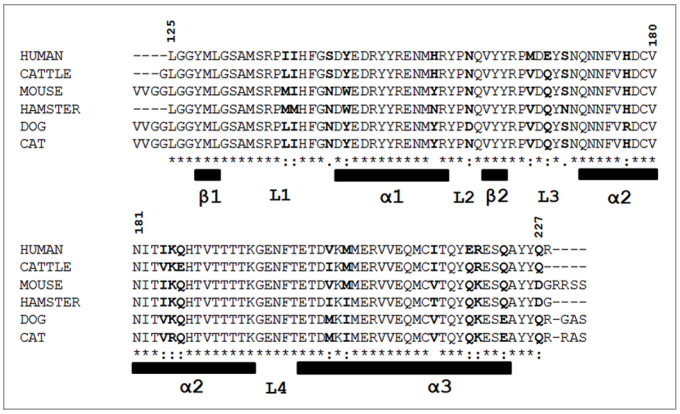

Figure 1. Amino acid sequences of C-terminal region of six mammalian prion proteins (PrPs). The six mammalian PrP sequences were compared. The bold residues are not conserved among the 6 PrPs. The residue numbering for all PrP was aligned with that for human PrP. The secondary structural element information was shown as α for α-helix, β for β-strand and L for loop or coil region.

loop has an important role in intermolecular interactions and it may be a key for PrP aggregation.[21] Still, no critical conformational differences have been identified that are linked to species barriers to prion transmission. An alternate approach is necessary to reveal the structural differences and/or differences in structural stability of PrP^C that exist among the different species.

The ab initio fragment molecular orbital (FMO) calculation is a powerful tool for quantum chemical analysis of intramolecular interactions in proteins and has been utilized to analyze protein-ligand binding affinities[22,23] and protein stabilities.[24-26] Intramolecular interactions between residues play a key role in the structural stability of proteins.[27] The intra- and inter-molecular interactions of mouse PrP models with explicit water has been examined using the FMO-RIMP2 method.[28] Using the FMO calculations, we previously demonstrated that the local structural stability of the E200K mutant of PrP was altered vis à vis that of the wild-type PrP. The instability of the E200K mutant structure is thought to be a trigger for conversion to PrP^{Sc}.[24]

In this study, we compared the intramolecular interactions of six mammalian PrPs ab initio to identify their structural differences, which were not detected by classical methods of structural determination. A clarification of the differences in intramolecular interactions between BSE-susceptible and BSE-resistant hosts may facilitate elucidation of the molecular mechanisms of species barriers to BSE prion transmission. Our calculations showed that canine and bovine PrP differ markedly in their local structural stabilities, providing a possible rationale for why canines and hamsters were resist to BSE infection.

Results

Structural comparison of PrP. The NMR structures of six mammalian PrPs were compared. Their amino acid sequences and secondary structures are shown in **Figure 1**. As reported previously,[16-20] the PrP backbone structures highly resemble one another (**Fig. 2A**). However, the orientation of PrP side chains is different, both on the outer surface and in the internal region (**Fig. 2B**), suggesting that the PrPs of all six animal species show differing intermolecular interactions and/or local structural stabilities.

FMO analysis of intramolecular interactions of PrP. To assess the intramolecular interactions of PrP, an FMO calculation was performed. The values of internal interaction energies (ΔE^{Int}) of nine secondary structural elements were negative, indicating the absence of clear differences among the animal species (**Table S1**). The values of the interfragment interaction energies (IFIEs) of residue pairs were negative or positive, denoting that the pairs were structurally stable or unstable, respectively. Since ΔE^{Int} is generated by summation of all of the IFIEs between the residues belonging to same element, this result suggests that each secondary element is structurally stable and primarily contributes to the similarity in backbone structure among the species. To compare the intramolecular interaction between secondary structural elements, we calculated the energies of 36 pair interactions (**Table 1**). As with IFIE and ΔE^{Int}, the pair interaction energy (ΔE^{Pair}) values were negative or positive, denoting that the pairs were structurally stable or unstable, respectively. It should be noted here that the interaction energies of ΔE^{Int} and ΔE^{Pair} provides information on local structural stabilities for the secondary structure elements of PrP but these energies are enthalpic contributions but not local folding free energies. Although partial unfolding free energies in some specified residues of PrP has been monitored by NMR,[29] present technique could not be used to analyze denaturation status of local elements of PrP. Therefore, there are no experimental data for verifying the obtained FMO calculations. The total ΔE^{Pair} for all species combined was negative, with similar values ranging from -618 to -794 kcal/mol. This result also suggests that the global structure for all PrPs is stable, irrespective of the animal species from which it originates. A maximum and a minimum value of ΔE^{Pair} within each examined animal species is shown in blue and red, respectively, in **Table 1**. As shown in **Table 1**, the ΔE^{Pair} values substantially differed between species on an individual basis. The seven elemental pairs, L1-α1, L1-L2, α1-L4, α1-α3, L3-α3, α2-L4 and α2-α3, showed substantially variability in their interaction energies among the animal species (σ > 20 kcal/mol; **Table 1**). Under mildly acidic pH conditions, the values of the two pairs (L1-α3 and α1-α2) also varied substantially (**Table S2**). These results indicate that the intramolecular interaction networks, specifically, the local structural stabilities, differed considerably among PrP species, despite their similarities in backbone structure. Notably, these differences were primarily caused by differences in minor amino acid residues and/or in structural orientations of side chains.

The interaction between α1 and α2 of BSE-susceptible animals (human, bovine, mouse and cat) ranged from -5 to -18 kcal/mol, whereas that of BSE-resistant animals was -24 kcal/mol (for hamster) and -30 kcal/mol (for dog). Similarly, the interaction between α2 and L4 of BSE-susceptible animals ranged from -48 to -71 kcal/mol and that of BSE-resistant animals was -90 kcal/mol (for dog) and -119 kcal/mol (for hamster). These results indicate that PrP from BSE-resistant animals

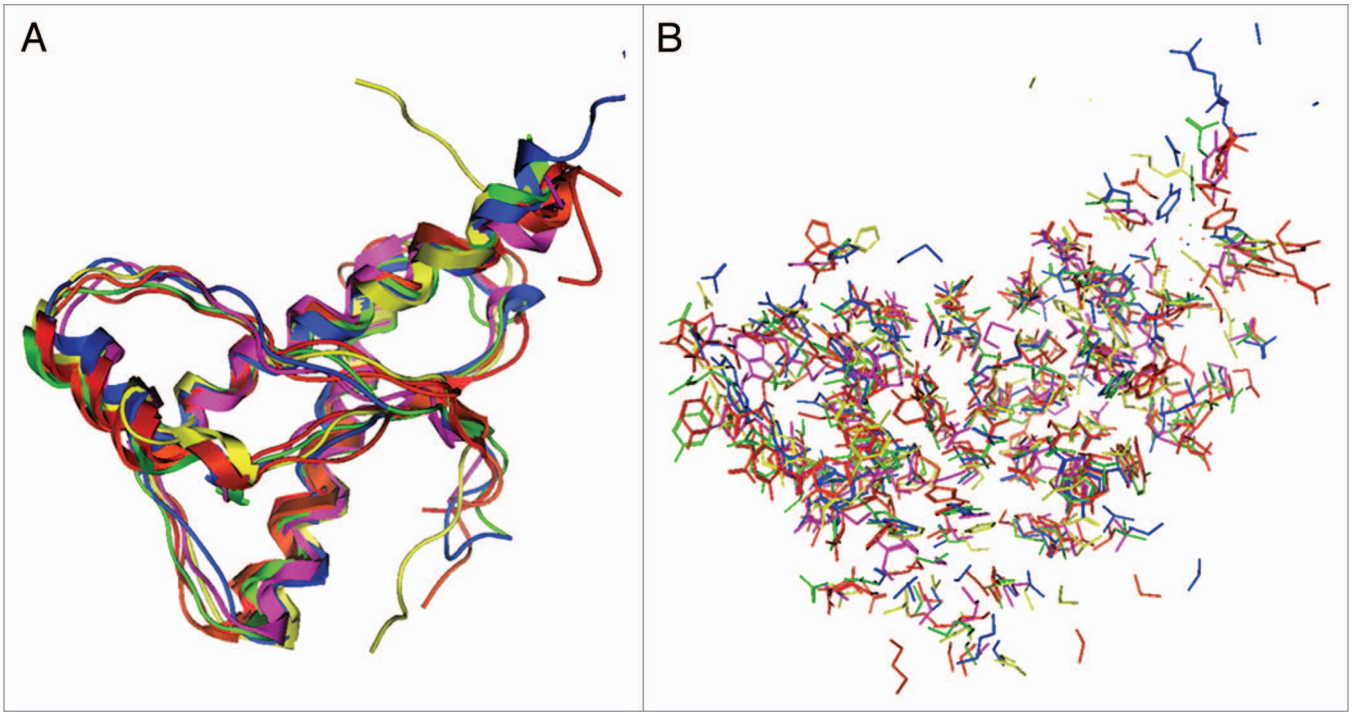

Figure 2. Superposition of the nuclear magnetic resonance (NMR) structures of 6 mammalian PrPs. The structures of backbone (**A**) and side chains (**B**) are illustrated: human (red), bovine (green), mouse (blue), hamster (purple), dog (yellow) and cat (orange).

maintains a relatively stable interaction in α1-α2 and α2-L4 regions (**Table 1**).

PCA for pair interaction energies (ΔE^{Pair}) of PrP. Principal component analysis (PCA) for the ΔE^{Pair} of animal PrP models under neutral and mildly acidic pH conditions was performed to clearly elucidate differences in ΔE^{Pair} values among animal PrPs. The coefficients of the eigenvector for the first principal component showed that ΔE^{Pair} differences were primarily attributable to 4 elemental pairs under neutral pH conditions: L1-α1, α1-L4, α2-L4 and α2-α3; and 6 element pairs under mildly acidic pH conditions L1-α1, L1-L2, α1-α2, α1-L4, α2-L4 and α2-α3 (**Table S2**). **Figure 3** shows the first principal component scores of the ΔE^{Pair} for the six animal PrPs in neutral and mildly acidic pH conditions. The PCA demonstrated that bovine and canine PrPs show markedly different local structural stabilities under neutral pH conditions. The interaction of the α2-α3 pair is significantly weaker in bovine PrP than in PrP of other animals and this difference may explain the peculiar interaction observed in bovine PrP (**Fig. 3**) and this pair energy might be one of the most important factor regarding the BSE sensitivity. The PCA score of the hamster PrP was plotted at a great distance from bovine PrP under mildly acidic pH conditions (**Fig. 3**). Higher principal components in the PCA did not identify any additional useful relationships (data not shown).

Discussion

During the transfer of prions from one species to another, complete failure of transmission or a greatly extended incubation period of affected animals is often encountered. Although the precise mechanisms of this species barrier phenomenon have not been fully elucidated, it is likely to have a biophysical basis in the structural differences between host PrP^{C} and PrP^{Sc} in the inoculum.[1] The conversion from PrP^{C} to PrP^{Sc} may be performed in multiple steps; a heterodimer of PrP^{C} and PrP^{Sc} has been purported to be generated initially.[1] A comparison of structural determinations of PrPs from different species may provide an insight into the susceptibility of a given species to interspecies prion transmission and into the nature of the species barrier.[30]

Although BSE prions have reportedly been transmitted to a wide range of animal species, dogs are known to be BSE-resistant animals.[13] It has also been reported that typical BSE was not transmitted to hamsters at the primary passage.[14] However, an atypical form of BSE known as the L-type BSE, was transmitted to hamsters at the primary passage.[31] This may imply that the resistance in hamsters to BSE prion infection is not absolute or even specific for typical BSE prions. We attempted to compare the structural differences among six mammalian PrPs based on their typical BSE susceptibility: four BSE-susceptible animals (cattle, cats, mice and humans) and two BSE-resistant animals (dogs and hamsters).

In this study, we demonstrated that the side-chain orientations of the PrP structures were species specific, irrespective of their similar backbone structures (**Fig. 2**). The geometrical differences in side-chain orientations in PrP caused by point mutations[29,32] or amino acid substitutions[17] have been investigated. These geometrical changes may affect critical intramolecular interactions in PrP. A quantitative evaluation of intramolecular interactions is essential in order to elucidate differences in PrP structural stability.

Table 1. The pair interaction energies (ΔE^{Pair}) of 6 mammalian PrP models under neutral pH condition

	Secondary Structure Element Pairs			Pair Interaction Energies, ΔE/kcal mol^{-1}							
				Human	Cattle	Mouse	Hamster	Dog	Cat	Average[a]	σ[b]
1	β1	–	L1	−29	−32	−34	−15	−24	−20	−26	7
2	β1	–	α1	+0	+0	−0	+0	−0	+0	+0	0
3	β1	–	L2	−1	+0	−2	−0	−0	−1	−1	1
4	β1	–	β2	−26	−22	−23	−16	−25	−35	−25	6
5	β1	–	L3	−29	−32	−17	−26	−25	−13	−24	7
6	β1	–	α2	+0	−2	−22	−5	−14	−2	−7	9
7	β1	–	L4	+0	−0	+0	−0	+0	+0	+0	0
8	β1	–	α3	−1	+2	−8	+2	−5	−4	−2	4
9	L1	–	α1	−123	−105	−133	−120	−84	−65	−105	26*
10	L1	–	L2	−55	−73	−34	−25	−83	−35	−51	23*
11	L1	–	β2	−9	−13	−14	−11	−15	−8	−12	3
12	L1	–	L3	−9	+3	+4	+4	+4	+4	+2	5
13	L1	–	α2	+19	+1	+15	+22	+34	+20	+18	10
14	L1	–	L4	−17	−25	−18	−22	−17	−19	−20	3
15	L1	–	α3	−99	−78	−52	−53	−90	−67	−73	19
16	α1	–	L2	−25	−33	−26	−24	−6	−27	−24	9
17	α1	–	β2	+1	+0	+0	−0	+0	+0	+0	0
18	α1	–	L3	+8	−1	−3	−2	−2	−1	−0	4
19	α1	–	α2	−16	−5	−15	−24	−30	−18	−18	8
20	α1	–	L4	−26	−65	−5	−4	+8	+6	−14	28*
21	α1	–	α3	−8	−11	−79	−22	+6	−49	−27	31*
22	L2	–	β2	−18	−27	−22	−22	−17	−14	−20	5
23	L2	–	L3	−0	+1	+1	+1	−3	+1	−0	2
24	L2	–	α2	−15	−14	−8	−25	−35	−6	−17	11
25	L2	–	L4	−1	−3	−1	−3	+19	+0	+2	8
26	L2	–	α3	−13	−4	−10	−9	+33	−9	−2	17
27	β2	–	L3	−12	−6	−12	−22	−12	−11	−13	5
28	β2	–	α2	−33	−7	−13	−21	−21	+2	−16	12
29	β2	–	L4	+1	+1	+1	+1	+1	+0	+1	0
30	β2	–	α3	−21	−20	−37	−27	−17	−9	−22	9
31	L3	–	α2	−45	−30	−42	−65	−31	−69	−47	17
32	L3	–	L4	+7	−2	−3	−3	−3	−2	−1	4
33	L3	–	α3	+42	−12	−19	−35	−12	−9	−7	26*
34	α2	–	L4	−71	−48	−62	−119	−90	−69	−77	25*
35	α2	–	α3	−89	−28	−56	−101	−160	−119	−92	47*
36	L4	–	α3	−12	−9	−11	−3	+19	+30	+2	18
	Total			−725	−699	−760	−794	−697	−618		

The pair interaction energies were evaluated by summation of the calculated IFIEs between the residues on the element pairs. [a]The average for the values of ΔE^{Pair}. [b]The standard deviations σ for the values of the ΔE^{Pair}. *The varied ΔE^{Pair} among the six mammalian PrP^C; σ ≥ 20 kcal/mol. The blue-marked boxes are the maximum values (i.e., most repulsive interaction) among the PrP species. The red-marked boxes are the minimum values (i.e., most attractive interaction) among the PrP species.

We compared the local structural stabilities of the secondary structural elements of mammalian PrP by FMO calculations. The structural stabilities of the elements were similar among all mammalian species (**Table S1**). However, our calculations show a considerably wide range of ΔE^{Pair} values in the specific local pairs and it indicates that the local structural stabilities varied among different animal species (**Table 1**). Since the magnitude of ΔE^{Pair} is indicative of the strength of the interaction, a negative value of ΔE^{Pair} denotes an attractive interaction (i.e., a structurally stable conformation), whereas a positive value denotes a repulsive interaction (i.e., a structurally unstable conformation). The stable pair regions are expected to be less susceptible to denaturation of structural conformation. These local regions could possess a highly variable internal local protein dynamics properties among the different animal species.

It is believed that the endosomes of scrapie-infected cells, characterized by mildly acidic pH conditions (pH 4.0–6.0), are the sites of PrP^{Sc} accumulation, while the cell surface, characterized by neutral pH conditions (~pH 7), is the site of PrP^C binding to PrP^{Sc}.[33] It has also reported that the endosomal recycling compartment is thought as the site of prion conversion.[34] Our calculations revealed that the local structural stabilities denoted by ΔE^{Pair} in the specific regions are markedly altered under lower pH conditions, an observation that highly depended on the animal species examined (**Table 1; Table S2**). Local structural stability of PrP varied with changes in pH conditions and no similarities among animal species were observed in association with pH alteration. This suggests that PrP^{Sc} conversion mechanisms differ depending on the animal species.

Our calculations also demonstrated that the total structural stabilities of the PrPs in different species were not directly related to their BSE susceptibilities and/or resistance, suggesting a greater importance for local structure of PrP in the elucidation of PrP denaturation properties. To clarify this difference among

animal species, we performed a PCA. The analysis clearly demonstrated that different structural stabilities exist between dog and cattle under neutral conditions and between hamster and cattle under mildly acidic conditions (**Fig. 3**). This observation suggests that different mechanisms underlie the resistance to BSE infection between dog and hamster. Our analysis showed that bovine PrP possessed markedly different characteristics from other PrPs, consistent with a previous observation that bovine PrP is more highly resistant to urea denaturation than are PrPs of other species.[29]

The peculiar local structural stabilities of bovine PrP was primarily derived by the weaker stability of the α2-α3 interaction. Furthermore, relatively weak interactions of α1-α2 and α2-L4 were observed in BSE-susceptible animals. These results may be explained by the hypothesis that PrP with weak interactions among α1, α2 and α3 sites could be converted to PrP^{Sc} by BSE prion infection. This may also account for the observation that resistance against proteolysis of PrP^{Sc} from BSE was weaker than that against scrapie.[35]

In conclusion, our FMO calculations revealed the different structural stabilities of PrP among different animal species. Cattle PrP has different biophysical characteristics from other mammalian PrPs. The results of this study suggest that differences in local structural stabilities of α1-α2 and α2-L4 of PrP provide a link to the mechanisms of species barriers against BSE prion infection.

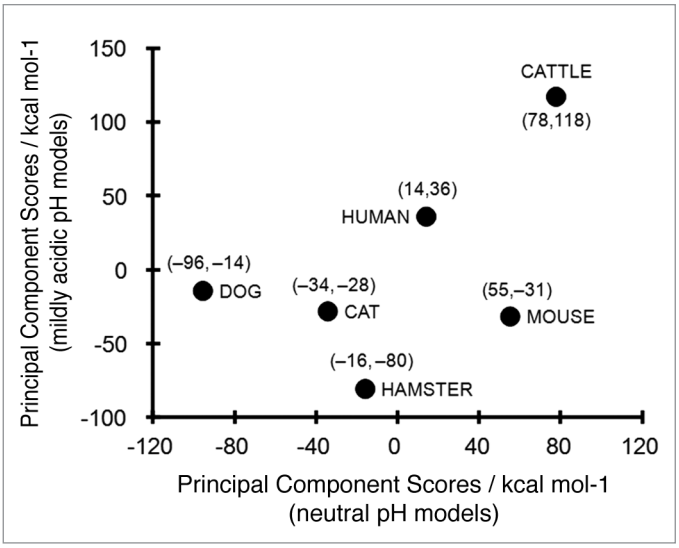

Figure 3. First principal component scores in the principal component analysis (PCA) for the ΔE^{Pair} of mammalian PrP. The scores under neutral (pH 7.0) and mildly acidic (pH 4.5) models were plotted in axes of abscissas and ordinates, respectively. The numerical values in the parenthesis are the scores for neutral pH and mildly acidic pH models, respectively.

Materials and Methods

Structural modeling of PrPs for FMO calculations. Initial atomic coordinates of mammalian PrP for human, cattle, mouse, hamster, dog and cat were extracted from the Protein Data Bank (PDB) structures with the codes 1QM3, 1DWZ, 1XYX, 1B10, 1XYK and 1XYJ, respectively. The residue numbering for all PrP species was identical to that of human PrP. The secondary structures of PrP were defined as follows: three α-helices (α1: 144–156, α2: 172–194 and α3: 200–223), two β-strands (β1: 129–131 and β2: 161–163) and four loop regions (L1: 132–143, L2: 157–160, L3: 164–171 and L4: 195–199) (**Fig. S1**). A multiple sequence alignment for the six PrPs was carried out using ClustalW (1.8.3 WWW Server in DNA Data Bank of Japan, National Institute of Genetics)[36] (**Fig. 1**). The PrP structural models were constructed for the top five conformers deposited in the PDB. For the neutral pH (pH 7.0) model of the PrPs as a cell surface model,[24] we made the following assumptions: (1) lysine, arginine and the N-terminal residues were positively charged; (2) glutamic acid, aspartic acid and the C-terminal residues were negatively charged; and (3) histidines were neutrally protonated at the Nτ atom. All other residues were considered to be neutrally charged. In the mildly acidic (pH 4.5) condition, the protonation states were identical to the pH 7.0, with the exception of histidines, in which the side chains were imidazolium forms and thus positively charged. The proteins in explicit water were modeled by arranging water molecules in a sphere within 16 Å of the protein surface. The geometric optimizations for protein models in water were performed using an AMBER99 force field with constraints of fixed heavy atoms in the whole protein, followed by restricting of the water molecules within 8 Å on the protein (1,489–1,913 molecules) for FMO calculations. Examples of solvated models are shown in **Figure S2**. The generated models were further optimized under constraints of fixed heavy atoms, with the exceptions of N- and C-terminal residues of the proteins. The modeling procedures were performed using MOE (version 2011.10, Chemical Computing Group, Inc.).

FMO calculations. Ab initio FMO calculations were carried out using the ABINIT-MP software (Advance/BioStation ver. 3.3, Advance Soft Corp.) with the RI-MP2 method[37,38] combined with the 6-31G basis set. In the FMO calculation, the protein models were fragmented into single amino acid residues, with the exception of the disulfide-bond residues of Cys176 and Cys214, which were considered a single fragment. The interfragment interaction energy (IFIE) between covalently adjoining residues were evaluated by subtracting the calculated IFIE from an IFIE between methyl groups in an ethylene molecule with a gauche form; this form has an identical C-C bond length with a bond length between a Cα atom and a backbone carbonyl C atom in the residues of the protein structure.[39] An average of the IFIEs was calculated for the top five conformer models. The pair interaction energy ΔE_{PQ}^{Pair} between the elements P and Q was evaluated using the following equation:

$$\Delta E_{PQ}^{Pair} = \sum_{I \in P} \sum_{J \in Q} \Delta E \quad (1)$$

where the ΔE_{IJ} is the IFIE between the I and J fragments in the P and Q elements, respectively. The internal interaction energy ΔE_{P}^{Int} for the element P was calculated using the following equation:

$$\Delta E_{P}^{Int} = \sum_{I \in P} \sum_{J \in P} \Delta E_{IJ} \quad (2)$$

The IFIE for the disulfide bond fragment was considered in the ΔE_{PQ}^{Pair} and ΔE_{P}^{Int} as described previously.[22] A typical run of a PrP model with explicit water took a calculation time of 10 hours on average using four quad-core AMD Opteron 2.5 GHz cluster (16 CPUs).

PCA. The PCA for the ΔE^{Pair} was performed by solving an eigenvalue problem for an actual variance-covariance matrix built from the variances of ΔE^{Pair}. The PCA was carried out using the statistical functions in the Microsoft Excel package (Microsoft Corp.). The principal component score of each animal species for the first principal component was obtained by calculating an inner product of the eigenvector for the first principal component and the vector whose components were the values that were generated by subtracting averaged ΔE^{Pair} over all species from ΔE^{Pair}.

Disclosure of Potential Conflicts of Interest

No potential conflicts of interest were disclosed.

Acknowledgments

The numerical calculations were supported by the Agriculture, Forestry and Fisheries Research Technology Center (AFFRIT). We thank Reiko Takeuchi for her general assistance. This study was supported by a grant-in-aid from the BSE and other Prion Disease Control Projects of the Ministry of Agriculture, Forestry and Fisheries, Japan.

Supplemental Materials

Supplemental materials may be found here:
www.landesbioscience.com/journals/prion/article/23122

References

1. Prusiner SB. Molecular biology of prion diseases. Science 1991; 252:1515-22; PMID:1675487; http://dx.doi.org/10.1126/science.1675487.
2. Moore RA, Vorberg I, Priola SA. Species barriers in prion diseases--brief review. Arch Virol Suppl 2005; 19:187-202; PMID:16355873.
3. Fraser H, Bruce ME, Chree A, McConnell I, Wells GA. Transmission of bovine spongiform encephalopathy and scrapie to mice. J Gen Virol 1992; 73:1891-7; PMID:1645134; http://dx.doi.org/10.1099/0022-1317-73-8-1891.
4. Foster JD, Hope J, Fraser H. Transmission of bovine spongiform encephalopathy to sheep and goats. Vet Rec 1993; 133:339-41; PMID:8236676; http://dx.doi.org/10.1136/vr.133.14.339.
5. Robinson MM, Hadlow WJ, Huff TP, Wells GA, Dawson M, Marsh RF, et al. Experimental infection of mink with bovine spongiform encephalopathy. J Gen Virol 1994; 75:2151-5; PMID:8077914; http://dx.doi.org/10.1099/0022-1317-75-9-2151.
6. Baker HF, Ridley RM, Wells GA, Ironside JW. Prion protein immunohistochemical staining in the brains of monkeys with transmissible spongiform encephalopathy. Neuropathol Appl Neurobiol 1998; 24:476-86; PMID:9888158; http://dx.doi.org/10.1046/j.1365-2990.1998.00142.x.
7. Lasmézas CI, Deslys JP, Demaimay R, Adjou KT, Lamoury F, Dormont D, et al. BSE transmission to macaques. Nature 1996; 381:743-4; PMID:8657276; http://dx.doi.org/10.1038/381743a0.
8. Bons N, Mestre-Frances N, Belli P, Cathala F, Gajdusek DC, Brown P. Natural and experimental oral infection of nonhuman primates by bovine spongiform encephalopathy agents. Proc Natl Acad Sci U S A 1999; 96:4046-51; PMID:10097160; http://dx.doi.org/10.1073/pnas.96.7.4046.
9. Wells GAH, Wilesmith JW. The neuropathology and epidemiology of bovine spongiform encephalopathy. Brain Pathol 1995; 5:91-103; PMID:7767494; http://dx.doi.org/10.1111/j.1750-3639.1995.tb00580.x.
10. Kirkwood JK, Cunningham AA. Epidemiological observations on spongiform encephalopathies in captive wild animals in the British Isles. Vet Rec 1994; 135:296-303; PMID:7817514; http://dx.doi.org/10.1136/vr.135.13.296.
11. Hewicker-Trautwein M, Bradley R. Portrait of transmissible feline spongiform encephalopathy. In: Hornlimann B, Riesner D, Kretzschmar H, eds. Prions in humans and animals. Berlin: Walter de Gruyter 2006:271-4.
12. Collinge J, Sidle KC, Meads J, Ironside J, Hill AF. Molecular analysis of prion strain variation and the aetiology of 'new variant' CJD. Nature 1996; 383:685-90; PMID:8878476; http://dx.doi.org/10.1038/383685a0.
13. Kirkwood JK, Cunningham AA. Epidemiological observations on spongiform encephalopathies in captive wild animals in the British Isles. Vet Rec 1994; 135:296-303; PMID:7817514; http://dx.doi.org/10.1136/vr.135.13.296.
14. Yokoyama T, Masujin K, Iwamaru Y, Imamura M, Mohri S. Alteration of the biological and biochemical characteristics of bovine spongiform encephalopathy prions during interspecies transmission in transgenic mice models. J Gen Virol 2009; 90:261-8; PMID:19088297; http://dx.doi.org/10.1099/vir.0.004754-0.
15. Wille H, Shanmugam M, Murugesu M, Ollesch J, Stubbs G, Long JR, et al. Surface charge of polyoxometalates modulates polymerization of the scrapie prion protein. Proc Natl Acad Sci U S A 2009; 106:3740-5; PMID:19223590; http://dx.doi.org/10.1073/pnas.0812770106.
16. Zahn R, Liu A, Lührs T, Riek R, von Schroetter C, López García F, et al. NMR solution structure of the human prion protein. Proc Natl Acad Sci U S A 2000; 97:145-50; PMID:10618385; http://dx.doi.org/10.1073/pnas.97.1.145.
17. Gossert AD, Bonjour S, Lysek DA, Fiorito F, Wüthrich K. Prion protein NMR structures of elk and of mouse/elk hybrids. Proc Natl Acad Sci U S A 2005; 102:646-50; PMID:15647363; http://dx.doi.org/10.1073/pnas.0409008102.
18. López Garcia F, Zahn R, Riek R, Wüthrich K. NMR structure of the bovine prion protein. Proc Natl Acad Sci U S A 2000; 97:8334-9; PMID:10899999; http://dx.doi.org/10.1073/pnas.97.15.8334.
19. Lysek DA, Schorn C, Nivon LG, Esteve-Moya V, Christen B, Calzolai L, et al. Prion protein NMR structures of cats, dogs, pigs, and sheep. Proc Natl Acad Sci U S A 2005; 102:640-5; PMID:15647367; http://dx.doi.org/10.1073/pnas.0408937102.
20. Liu H, Farr-Jones S, Ulyanov NB, Llinas M, Marqusee S, Groth D, et al. Solution structure of Syrian hamster prion protein rPrP(90-231). Biochemistry 1999; 38:5362-77; PMID:10220323; http://dx.doi.org/10.1021/bi982878x.
21. Sigurdson CJ, Joshi-Barr S, Bett C, Winson O, Manco G, Schwarz P, et al. Spongiform encephalopathy in transgenic mice expressing a point mutation in the β2-α2 loop of the prion protein. J Neurosci 2011; 31:13840-7; PMID:21957246; http://dx.doi.org/10.1523/JNEUROSCI.3504-11.2011.
22. Fukuzawa K, Mochizuki Y, Tanaka S, Kitaura K, Nakano T. Molecular interactions between estrogen receptor and its ligand studied by the ab initio fragment molecular orbital method. J Phys Chem B 2006; 110:16102-10; PMID:16898767; http://dx.doi.org/10.1021/jp060770i.
23. Sawada T, Hashimoto T, Nakano H, Suzuki T, Suzuki Y, Kawaoka Y, et al. Influenza viral hemagglutinin complicated shape is advantageous to its binding affinity for sialosaccharide receptor. Biochem Biophys Res Commun 2007; 355:6-9; PMID:17292854; http://dx.doi.org/10.1016/j.bbrc.2006.12.239.
24. Hasegawa K, Mohri S, Yokoyama T. Fragment molecular orbital calculations reveal that the E200K mutation markedly alters local structural stability in the human prion protein. Prion 2010; 4:38-44; PMID:20139714; http://dx.doi.org/10.4161/pri.4.1.10890.
25. Ishikawa T, Ishikura T, Kuwata K. Theoretical study of the prion protein based on the fragment molecular orbital method. J Comput Chem 2009; 30:2594-601; PMID:19408278; http://dx.doi.org/10.1002/jcc.21265.
26. Fukuzawa K, Komeiji Y, Mochizuki Y, Kato A, Nakano T, Tanaka S. Intra- and intermolecular interactions between cyclic-AMP receptor protein and DNA: ab initio fragment molecular orbital study. J Comput Chem 2006; 27:948-60; PMID:16586530; http://dx.doi.org/10.1002/jcc.20399.
27. Stites WE. Protein-protein Interactions: Interface Structure, Binding Thermodynamics, and Mutational Analysis. Chem Rev 1997; 97:1233-50; PMID:11851449; http://dx.doi.org/10.1021/cr960387h.
28. Ishikawa T, Kuwata K. Interaction analysis of the native structure of prion protein with quantum chemical calculations. J Chem Theory Comput 2010; 6:538-47; http://dx.doi.org/10.1021/ct900456v.
29. Julien O, Chatterjee S, Bjorndahl TC, Sweeting B, Acharya S, Semenchenko V, et al. Relative and regional stabilities of the hamster, mouse, rabbit, and bovine prion proteins toward urea unfolding assessed by nuclear magnetic resonance and circular dichroism spectroscopies. Biochemistry 2011; 50:7536-45; PMID:21800884; http://dx.doi.org/10.1021/bi200731e.
30. Schwarzinger S, Willbold D, Ziegler J. Structural studies of prion proteins. In: Hornlimann B, Riesner D, Kretzschmar H, eds. Prions in humans and animals. Berlin: Walter de Gruyter 2006:79-94.
31. Shu YJ, Masujin K, Okada H, Iwamaru Y, Imamura M, Matsuura Y, et al. Characterization of Syrian hamster adapted prions derived from L-type and C-type bovine spongiform encephalopathies. Prion 2011; 5:103-8; PMID:21597334; http://dx.doi.org/10.4161/pri.5.2.15847.
32. Calzolai L, Lysek DA, Guntert P, von Schroetter C, Riek R, Zahn R, et al. NMR structures of three single-residue variants of the human prion protein. Proc Natl Acad Sci U S A 2000; 97:8340-5; PMID:10900000; http://dx.doi.org/10.1073/pnas.97.15.8340.
33. Borchelt DR, Taraboulos A, Prusiner SB. Evidence for synthesis of scrapie prion proteins in the endocytic pathway. J Biol Chem 1992; 267:16188-99; PMID:1353761.

34. Marijanovic Z, Caputo A, Campana V, Zurzolo C. Identification of an intracellular site of prion conversion. PLoS Pathog 2009; 5:e1000426; PMID:19424437; http://dx.doi.org/10.1371/journal.ppat.1000426.
35. Kuczius T, Groschup MH. Differences in proteinase K resistance and neuronal deposition of abnormal prion proteins characterize bovine spongiform encephalopathy (BSE) and scrapie strains. Mol Med 1999; 5:406-18; PMID:10415165.
36. Thompson JD, Higgins DG, Gibson TJ. CLUSTAL W: improving the sensitivity of progressive multiple sequence alignment through sequence weighting, position-specific gap penalties and weight matrix choice. Nucleic Acids Res 1994; 22:4673-80; PMID:7984417; http://dx.doi.org/10.1093/nar/22.22.4673.
37. Ten-no S, Iwata S. Three-center expansion of electron repulsion integrals with linear combination of atomic electron distributions. Chem Phys Lett 1995; 240:578-84; http://dx.doi.org/10.1016/0009-2614(95)00564-K.
38. Ten-no S, Iwata S. Multiconfiguration self-consistent field procedure employing linear combination of atomic-electron distributions. J Chem Phys 1996; 105:3604-11; http://dx.doi.org/10.1063/1.472231.
39. Fedorov DG, Kitaura K. Pair interaction energy decomposition analysis. J Comput Chem 2007; 28:222-37; PMID:17109433; http://dx.doi.org/10.1002/jcc.20496.